Lawrence Berkeley Laboratory
UNIVERSITY OF CALIFORNIA

Physics Division

Submitted to Radio Science

ATMOSPHERIC EMISSION VARIATION MEASUREMENTS
AT 3, 0.9, and 0.33 cm WAVELENGTH

G.F. Smoot, S.M. Levin, G. De Amici, and
C. Witebsky

May 1985

Prepared for the U.S. Department of Energy under Contract DE-AC03-76SF00098

DISCLAIMER

LBL-19622

Atmospheric Emission Variation Measurements at 3, 0.9, and 0.33 cm Wavelength

G.F. Smoot, S.M. Levin, G. De Amici, and C. Witebsky

Space Sciences Laboratory
and
Lawrence Berkeley Laboratory
University of California
Berkeley, California 94720

May 1985

Atmospheric Emission Variation Measurements at 3, 0.9, and 0.33 cm Wavelength

G. F. Smoot, S. M. Levin, G. De Amici, and C. Witebsky
Space Sciences Laboratory and Lawrence Berkeley Laboratory, University of California

ABSTRACT

We have measured the fluctuation power spectrum and correlation of fluctuations of atmospheric emission at wavelengths of 3, 0.9, and 0.33 cm. The fluctuations are well correlated and can be described with a simple parameterization. Our results are in agreement with other measurements of phase and absorption variation and with the hypothesis that atmospheric water fluctuations dominate other effects. The measurements are in good agreement with the predictions of the Kolmogorov turbulence theory, which can be used to predict the temporal and spatial spectra of atmospheric scintillation and emission variation.

1. INTRODUCTION

There have been many measurements of the limitations on radio and microwave systems imposed by atmospheric variation. In communication systems atmospheric scintillation appears to be the most important limitation, while in remote sensing, astronomy, and other radiometric applications emission variation is the most important effect. In general the one most significant cause is the variation in the amount of atmospheric water (H_2O). The most obvious effects are those induced by weather and extreme meteorological conditions. The conditions that affect radio and microwave signals span the range from thundershowers and weather fronts to local evaporation. Figure 1 is a summary of the attenuation of the atmosphere for a number of different atmospheric conditions.

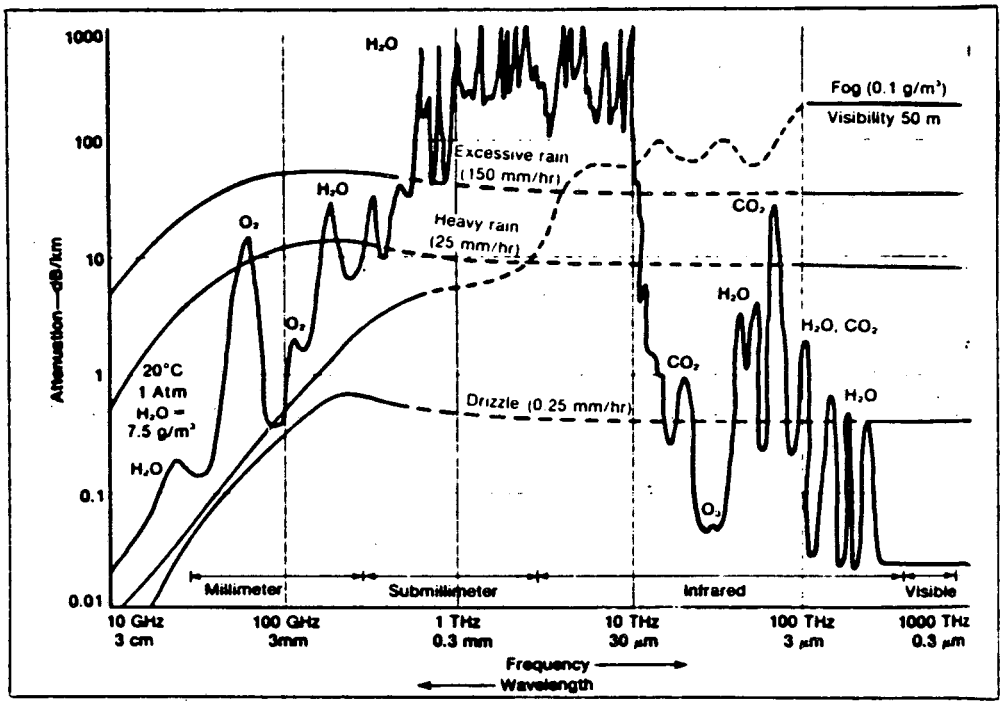

Figure 1. Attenuation (db/km) versus Frequency.
Reproduced from Microwave & RF, Vol 26, No. 9, page 64.

This paper presents new measurements of atmospheric water variation and its effects as measured in the microwave region. It also summarises the results of previous measurements and interprets the data in the context of the Kolmogorov turbulence theory.

2. THEORY

It appears that the results of all published measurements can be reasonably explained as primarily resulting from variations in the atmospheric water content. This is what is expected because the other major microwave emitter, O_2, is well mixed in the atmosphere. Changes in O_2 emission generally track the barometric pressure, since temperature variations tend to be compensated for by the corresponding density variation. One must realise that at very short wavelengths, e.g. visible light, and under special surface conditions temperature gradients and convection cells can produce refraction related effects such as scintillation, fading, and ducting. Interestingly, the optical phase variation spectrum appears to match with the water variation effect.

The data are often taken in diverse parameters: phase variation, time delay, or as signal fluctuations. Accordingly, we have converted all the data into equivalent RMS atmospheric water column density fluctuations so that the results will be independent of wavelength and method. The relationship we have used for time delay is:

$$\Delta t = \frac{(n-1)}{c}\Delta \mathrm{H_2O}, \tag{1a}$$

For phase variation we used:

$$\Delta\phi(t,D) = \frac{2\pi}{\lambda}(n-1)\Delta \mathrm{H_2O}, \tag{1b}$$

where n = 1.33 is the index of refraction, ΔH_2O is the variation in column density of water (e.g. equivalent depth of liquid), and λ is the wavelength. The signal variations due to absorption or emission have been converted to equivalent RMS atmospheric water column density variations by using either the measured coefficients for each frequency or those calculated by the theories of Waters or Liebe (Costales *et al.* 1985). Sample coefficients for 10, 33, and 90 GHz at sea level are 0.65, 5.2, and 29 K/cm respectively.

The Kolmogorov turbulence theory provides a framework for comparing and organizing the data. The Kolmogorov model (Tatarski, 1960) predicts that the power spectra of atmospheric water fluctuations is given by:

$$|P(\mathrm{H_2O})|^2 = C^2 D^{\alpha} \tag{2}$$

where α is the power-law exponent, C is the normalization coefficient of the structure function, and D is the physical separation. In the Kolmogorov theory α is expected to be about 5/3 for distances less than the height of the troposphere (about 5.6 km), where turbulence is fully developed, and about 2/3 for larger scales where the turbulence is restricted to two dimensions. Dravskikh and Finkelstein (1979) quote another break to a flat spectrum for separations larger than 3000 km. The conversion from spatial dependence to time dependence generally rests on the assumption that the turbulence is mechanically transported by the wind and that the wind has a mean velocity, so that one can substitute $v_{wind}t$ for D. While the Kolmogorov theory is derived for mechanical turbulence in the atmosphere, one would expect water to be a good tracer of the turbulence and have similar behavior. Therefore we have the description:

$$\begin{aligned} |P(\mathrm{H_2O})|^2 &= C^2 f^{-(\alpha+1)} D^{\alpha} && && (2') \\ &= {C_1}^2 f^{-8/3} D^{5/3} && 10\ \mathrm{cm} < D < 5.6\ \mathrm{km} && (2a') \\ &= {C_2}^2 f^{-5/3} D^{2/3} && 5.6\ \mathrm{km} < D < 3000\ \mathrm{km} && (2b') \end{aligned}$$

where the frequency dependence holds for temporal spectra and the distance dependence holds for spatial separation. The lower limit of the validity of equation (2a') is set by the physical size of the equipment and the wavelength because diffraction and averaging become important; 10 cm is a typical scale.

In order to convert the power spectra to the RMS variation in the atmospheric water column density we multiply by the frequency and take the square root:

$$\begin{aligned} <(\mathrm{H_2O})^2>^{1/2} &= C f^{-\alpha/2} D^{\alpha/2} && && (3) \\ &= C_1 f^{-0.833} D^{0.833} && D < 5.6\ \mathrm{km} && (3a) \\ &= C_2 f^{-0.333} D^{0.333} && D > 5.6\ \mathrm{km} && (3b) \end{aligned}$$

We have fitted and parameterized our measurements and other published data as described above. The results are summarized in Table 1.

Source	Location	Sampling Range (seconds)	RMS Variation σ_{H_2O} (cm) t in seconds; D in meters
Smoot *et al.*	Berkeley	$1 \leq t \leq 4096$	$(5. \pm 2.5) \times 10^{-3} t^{0.6 \pm 0.3}$
Thompson *et al.*	Hawaii	$1 \leq t \leq 2400$	$(5.6 \pm 2.5) \times 10^{-3} t^{0.8 \pm 0.1}$
Hogg *et al.*	Denver	$120 < t < 10^5$	$(2. \pm 1.6) \times 10^{-3} t^{0.6 \pm 0.2}$
Armstrong and Sramek	New Mexico	$10^4 \leq t \leq 10^6$ 1 km $\leq D \leq$ 35 km	$(8 \pm 8) \times 10^{-3} D^{0.7 \pm 0.2}$
Bieging *et al.*	Hat Creek, CA	$50 \leq t \leq 500$ 12 m $\leq D \leq$ 150 m	$(3 \pm 3) \times 10^{-3} D^{0.833}$
Dravskikh & Finkelstein		$1 \leq t \leq 10^5$ 100 m $\leq D \leq$ 5 km	$(3 \pm 2) \times 10^{-3} D^{0.833}$
Hinder	Cambridge, England	$20 \leq t \leq 10^5$ 50 m $\leq D \leq$ 1600 m	$(13.5 \pm 2.4) \times 10^{-3} D^{0.6 \pm 0.4}$ $(2.3 \pm 0.5) \times 10^{-3} D^{0.833}$
Basart *et al.*	West Virginia	$15 \leq t \leq 2000$ 200 m $\leq D \leq$ 11.3 km	$(21. \pm 16) \times 10^{-3} D^{0.4 \pm 0.1}$ $(0.6 \pm 0.2) \times 10^{-3} D^{0.833}$
Baars	West Virginia	$15 \leq t \leq 2000$ 2100 m $\leq D \leq$ 2700 m	$(1.6 \pm 0.6) \times 10^{-3} D^{0.833}$

Table 1: Measurements of RMS Variations in H_2O

The turbulence shows up both in the evolution of the atmospheric water irregularities and by the transport of these irregularities which comove with the airmass. Observations of clouds indicate that wind transport is usually the dominant effect in causing liquid water and water vapor variations in comparison to structural evolution. The data are well fit by the approximation that the water variations along the line of sight are produced by mechanical transport of irregularities. Measurements by several observers indicate that this description is valid in the centimeter wavelength range (Richaria 1985).

3. THESE MEASUREMENTS

We made a series of measurements at 10, 33, and 90 GHz (3, 0.9, and 0.33 cm wavelength) of the time variation of the atmospheric emission. The radiometers used were superheterodyne, Dicke-switched receivers. Three of the radiometers used low-side-lobe horn antennas with a half-power beam width of 7.5°. For most measurements the radiometers were aligned so that one antenna pointed vertically while the other pointed south at an angle of 40° from the vertical. An additional radiometer operated at 31.4 GHz (0.9 cm wavelength) had two beams with half-power widths of 0.5° and a separation of 1.7°. The radiometers were sufficiently stable that the fluctuations in output were dominated by variations in atmospheric emission except on short time scales where the radiometer noise was important.

Sample data from our measurements are shown in Figures 2 through 5. Figure 6 is a set of scatter plots showing the correlation of fluctuations in sky temperature observed simultaneously by the three co-aligned radiometers. The covariance is significant when one takes into account the intrinsic noise of the radiometers. The correlation coefficients for 10 and 33 GHz and 33 and 90 GHz are similar to those expected from water vapor variation and the absolute emission measurements at these frequencies (Costales, *et al.* 1985).

In our data one expects a break in the turbulence power spectrum at a time scale corresponding to the time that the evolving water structures take to travel from one beam to the other. For example, at a wind speed of 2 m/sec (4 mph) the transport time from one beam center to the other (angular separation, $\delta\theta$, of 1.7° or 40°) for an atmospheric water scale height of 2.2 km, is given by:

$$\Delta t = \frac{2.2\ \text{km}}{2\ \text{m/sec}} \delta\theta \sec(z)$$
$$= 32 \sec(z)\ \text{seconds}$$

for the $\delta\theta = 1.7°$ separation of the 31.4 GHz system observing at zenith angle z, and

$$\Delta t = 600\ \text{seconds}$$

for the $\delta\theta = 40°$ of the other three radiometers. We regularly see such a break in the 31.4 GHz data, since each spectral measurement usually lasts at least an hour. However, fewer of the samples from the other frequencies show a clear break as most of the individual spectra cut off at a frequency of 1/1024 Hz, not providing sufficient baseline for a careful observation.

4. TIME VARIATION RESULTS

The temporal power spectra of the atmospheric water variation as measured in different experiments is shown in Figure 7. The slope of the data on the plot should be compared to the theoretical Kolmogorov exponent, $\alpha + 1$, of 8/3. A line with this slope matches the data well; however, different sections of the data seem to have a different normalization or overall scale for the amount of H_2O. These shifts may well be due to normal seasonal and geographical climate effects. In our judgment there is no evidence for the expected deviations and breaks in the spectra. The structure in the data is consistent with what one would normally expect from a limited data set. Averaging over several spectra seems to produce smoothing to a single slope.

5. SPATIAL VARIATIONS IN THE ATMOSPHERE

The data converted to RMS fluctuations in atmospheric water are plotted versus separation in Figure 8. Figure 8 also shows two power-law lines with the Kolmogorov theory exponents to help guide the eye. The data on spatial variation are not very extensive or well controlled and therefore do not test the theory well. The theory does appear adequate as a rough estimator and may well be accurate.

6. SUMMARY, INTERPRETATION, AND PREDICTIONS

Given the overall variation in general climatic conditions we can conclude that most of the observed variation in the microwave properties of the atmosphere is due to the variation in H_2O and that the Kolmogorov theory gives a good description of its behavior. One should note that the best test of the theory is in the time spectra, while the spatial spectrum, which is more fundamental to the theory, is not well tested. If one can set the amplitude scale for the location and time of interest, one can predict the behavior of the atmospheric variations over a very large range in wavelengths and time scales. The simple parameterization provides a good estimate of atmospheric effects.

It is valid to use these data for predictions of phase scintillations and time delay fluctuations. However one must exercise more care when estimating emission and absorption fluctuations if one is operating at a frequency near a water-vapor line where the conversion of water vapor to liquid water makes a significant opacity change. This use of Kolmogorov turbulence theory does not explicitly include phase transitions that change the ratio of liquid to vapor, which could cause a significant change in the atmospheric opacity. At 10, 33, and 90 GHz, the frequencies of these observations, the vapor and liquid have nearly the same relative coefficients, so this effect is relatively small. Thus the radiometer outputs correlate for clouds as well as for vapor variations.

Acknowledgements: We thank Jon Aymon, Hal Dougherty, John Gibson, Janice Gates, and Faye Mitschang for their assistance. We gratefully acknowledge the encouragment, support, and interest shown by Herb Pascalar, John Brown, and their associates at Aerojet ElectroSystems.

This research was supported in part by National Science Foundation Grants No. PHY80-15694 and AST 800737, by the Department of Energy under Contract DE-AC03-76SF00098, by the California Space Group, and by the Italian Consiglio Nazionale delle Ricerche and CNR Fellowships No. 203.2.13 and 203.2.15, by Italian Ministero Della Pubblica Istruzione, and by NATO Grant 1871.

REFERENCES

Altshuler, E.E., M.A. Gallop, and L.E. Telford (1978), Atmospheric attenuation statistics at 15 and 35 GHz for very low elevation angles, Radio Science, 13, 5, 839-852.

Armstrong, J.W., and R.A. Sramek (1982), Observations of tropospheric phase scintillations at 5 GHz on vertical paths, Radio Science, 17 (6), 1579-1586

Baars, J.W.M. (1967), Meteorological influences on radio interferometer phase fluctuations, IEEE Trans. Antennas and Propagations, AP-15, 582-584.

Basart, J.P., G.K. Miley, and B.G. Clark (1970), Phase measurements with an interferometer baseline of 11.3 km, IEEE Trans. Antennas and Propagation AP-18, 375-379

Bieging, J.H., J. Morgan, W.J. Welch, S.N. Vogel, and M.C.H. Wright (1984), Interferometric Measurements of Atmospheric Phase Noise at 86 GHz, Radio Science, xx,yy.

Costales, J., Smoot, G.F., Witebsky, C., De Amici, G., Friedman, S. 1985), Simultaneous Measurements of Atmospheric Emission at 10, 33, and 90 GHz, Radio Science, xx,yy.

Dravskikh, A.F., and A.M. Finkelstein, (1979), Tropospheric limitations in phase and frequency coordinate measurements in astronomy, Astrophys. Space Sciences, 60, 251.

Hinder, R.A. (1969), Observations of atmospheric turbulence with a radio telescope at 5 GHz, Nature, 225, 614-617.

Hinder, R.A. and M. Ryle (1971), Atmospheric limitations to the angular resolution of aperture synthesis radio telescopes, Mon. Not. Royal Astron. Soc., 154, 229-253.

Flock, W.L., S.D. Slobin and E.K. Smith (1982), Propagation effects on radio range and noise in earth-space telecomunications, Radio Science, V. 17, 6, 1411-1424 Nov-Dec 1982.

Hogg, D.C., F.O. Guiraud, and M.T. Decker (1981), Measurement of excess radio transmission length on earth-space paths, Astron. Astrophys., 95, 304-307.

Hogg, D.C., F.O. Guiraud, and W.B. Sweezy (1981b), The short- term temporal spectrum of precipitable water vapor, Science, 213, 1112.

Lo, Lai-iun, Bob M. Fannin and Archie W. Straiton (1975), Attenuation of 8.6 and 3.2 mm Radio Waves by Clouds, IEEE Trans. Antennas Propag., AP-23, 6, 782-786.

Richaria, M., (1985), Simulate Tropospheric Amplitude Scintillation, Microwaves & RF, V. 24, 479.

Slobin, S.D., Microwave noise temperature and attenuation of clouds: Statistics of these effects at various sites in the United States, Alaska and Hawaii, Radio Science, V. 17,6, 1443-1454, Nov-Dec 1982.

Smith, E.K., Centimeter and millimeter wave attenuation and brightness temperature due to atmospheric oxygen and water vapor, Radio Science, V. 17, 6, 1455-1464, Nov-Dec 1982.

Tatarski, V.I. (1960) Wave Propagation in a Turbulent Medium (Translated from Russian), New York

Thompson, M.C., L.E. Wood, H.B. Janes, and D. Smith (1975), Phase and amplitude scintillations in the 10 to 40 GHz band, IEEE Trans. Antennas Propag., AP-23,792.

FIGURE CAPTIONS

Figure 1. Attenuation (db/km) versus Frequency. Reproduced from Microwave & RF, Vol 26, No. 9, page 64.

Figure 2. Sample Data from the 10, 33 and 90 GHz Radiometers. Times series of data with a one second sample. The data show granularity due to the ADC digitization and differential non-linearity. a) Data taken during poor weather on 22 October 1983 b) Data taken during good weather on 21 October 1983.

Figure 3. Composite Fourier transform of data from four days (21, 22, 26, and 27 October 1983) showing spectra of fluctuations. The flat portion of the spectra on the right hand side is the region dominated by the radiometer noise.

Figure 4. Sample Data from the 31.4 GHz Radiometer. Times series of data with a one second sample. The data show slight granularity due to the ADC digitization and differential non-linearity. Three different days are shown: a) March 9, 1984; a bad weather sample; very cloudy and foggy, b) February 29, 1984; partly cloudy atmospheric conditions sample , c) May 6, 1984; a clear weather sample. These data are all taken at a zenith angle of 40°. It is coincidental that the samples happen to have their small fluctuations at the beginning of the runs. Other samples have relative quiet at different times. The structure coincides with the passage of clouds through the beam.

Figure 5. Sample Data from the 31.4 GHz Radiometer. Fourier Transform of data showing spectra of fluctuations. Data samples a, b, c, are the same as shown in figure 4.

Figure 6. Correlation in Fluctuations of Atmospheric Signal From One Frequency to Another. a) 10 vs 33 GHz, b) 33 vs 90 GHz, c) 10 vs 90 GHz.

Figure 7. Power Spectra of Water Fluctuations. The dotted spectra are from *Hogg et al.*[1981]. The dashed line is the equivalent temporal spectrum inferred for the data of *Dravskikh and Finkelstein* [1979] according to the work of *Armstrong and Sramek* [1982] whose data are shown as the shaded box. The solid line is a sample of our data. Inclusion of all our data would produce a set of lines with slightly different slopes and relative heights of $\pm$ 50%. The +'s connected by the solid line are the converted phase (time delay) data of *Thompson et al.*[1975]. The dot-dash line indicates the optical data of *Shannon et al.*[1979].

Figure 8. RMS Atmospheric Water Fluctuation versus Separation D. The dotted lines show the expected slopes for the two regimes. Unfortunately, the data come from different geographical locations and different seasons. The open circles show data from Cambridge, England; the higher values were obtained in the summer and the lower in winter. New Mexico is a drier site than England. Within their typical variation and accounting for geography the data are consistent with Kolmogorov turbulence theory.

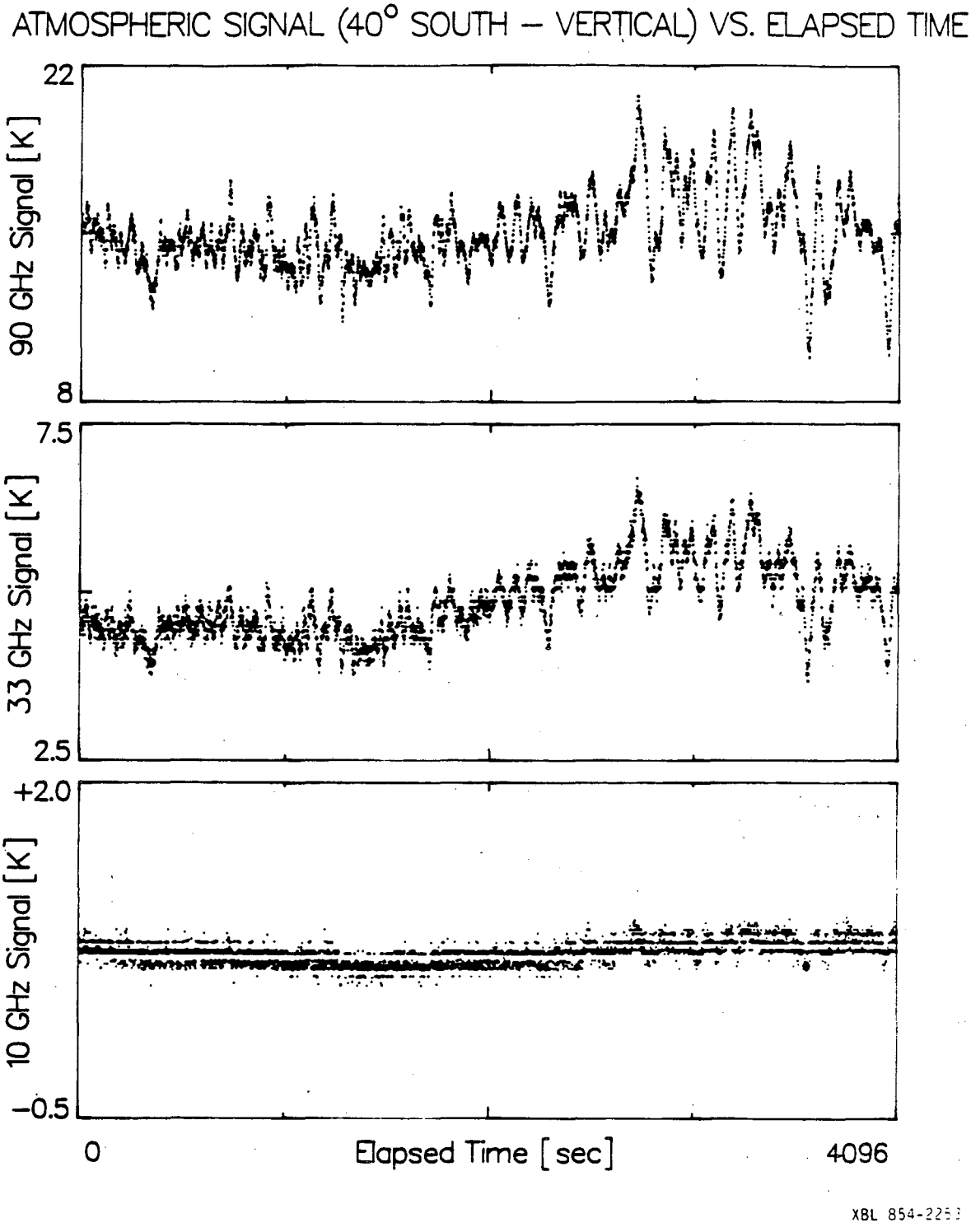

Figure 2. Sample Data from the 10, 33 and 90 GHz Radiometers. Times series of data with a one second sample. The data show granularity due to the ADC digitization and differential non-linearity. a) Data taken during poor weather on 22 October 1983

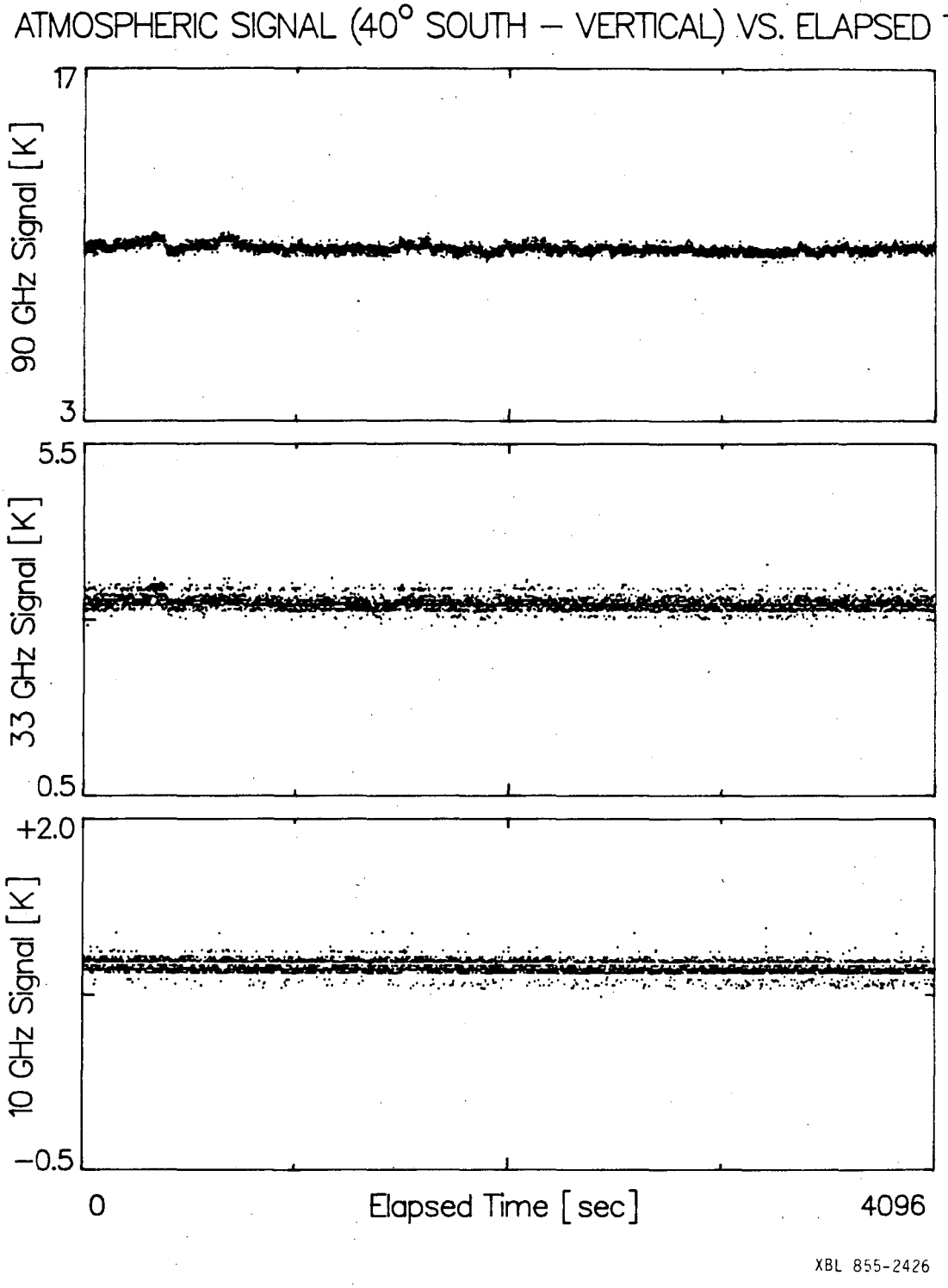

2 b) Data taken during good weather on 21 Ocotber 1983

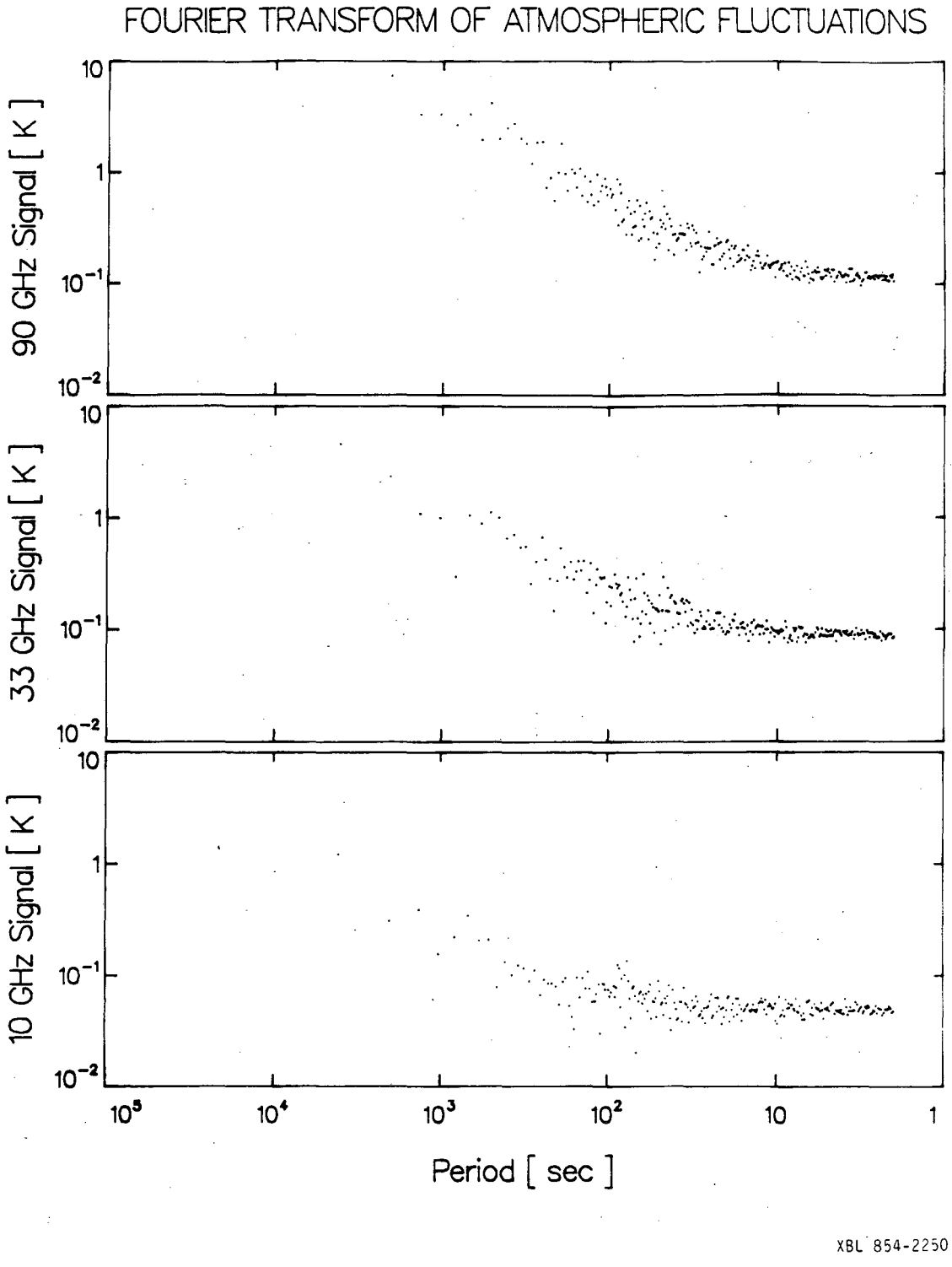

Figure 3. Composite Fourier transform of data from four days (21, 22, 26, and 27 October 1983) showing spectra of fluctuations. The flat portion of the spectra on the right hand side is the region dominated by the radiometer noise.

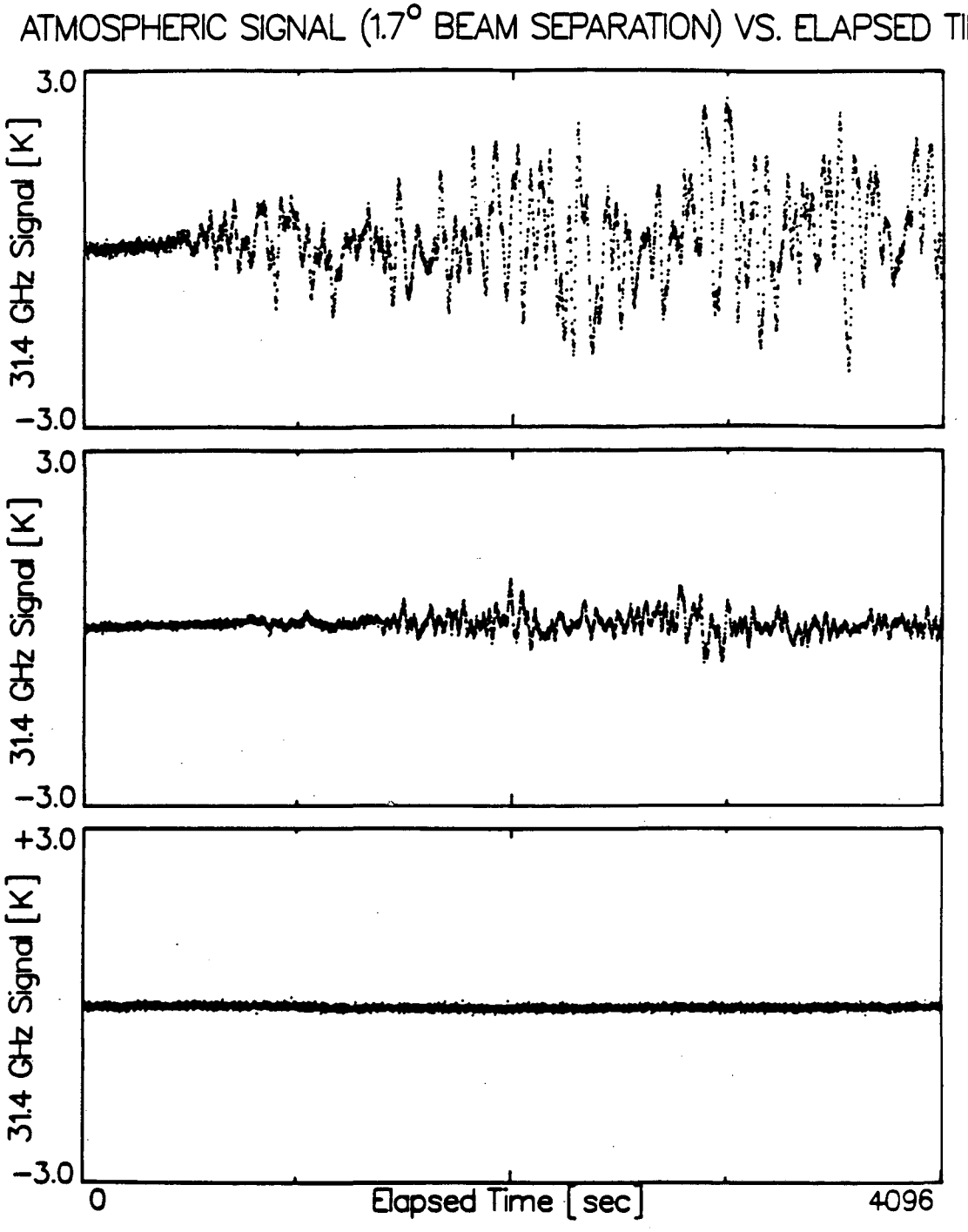

Figure 4. Sample Data from the 31.4 GHz Radiometer. Times series of data with a one second sample. The data show slight granularity due to the ADC digitization and differential non-linearity. Three different days are shown: a) March 9, 1984; a bad weather sample; very cloudy and foggy, b) February 29, 1984; partly cloudy atmospheric conditions sample , c) May 6, 1984; a clear weather sample. These data are all taken at a zenith angle of 40°. It is coincidental that the samples happen to have their small fluctuations at the beginning of the runs. Other samples have relative quiet at different times. The structure coincides with the passage of clouds through the beam.

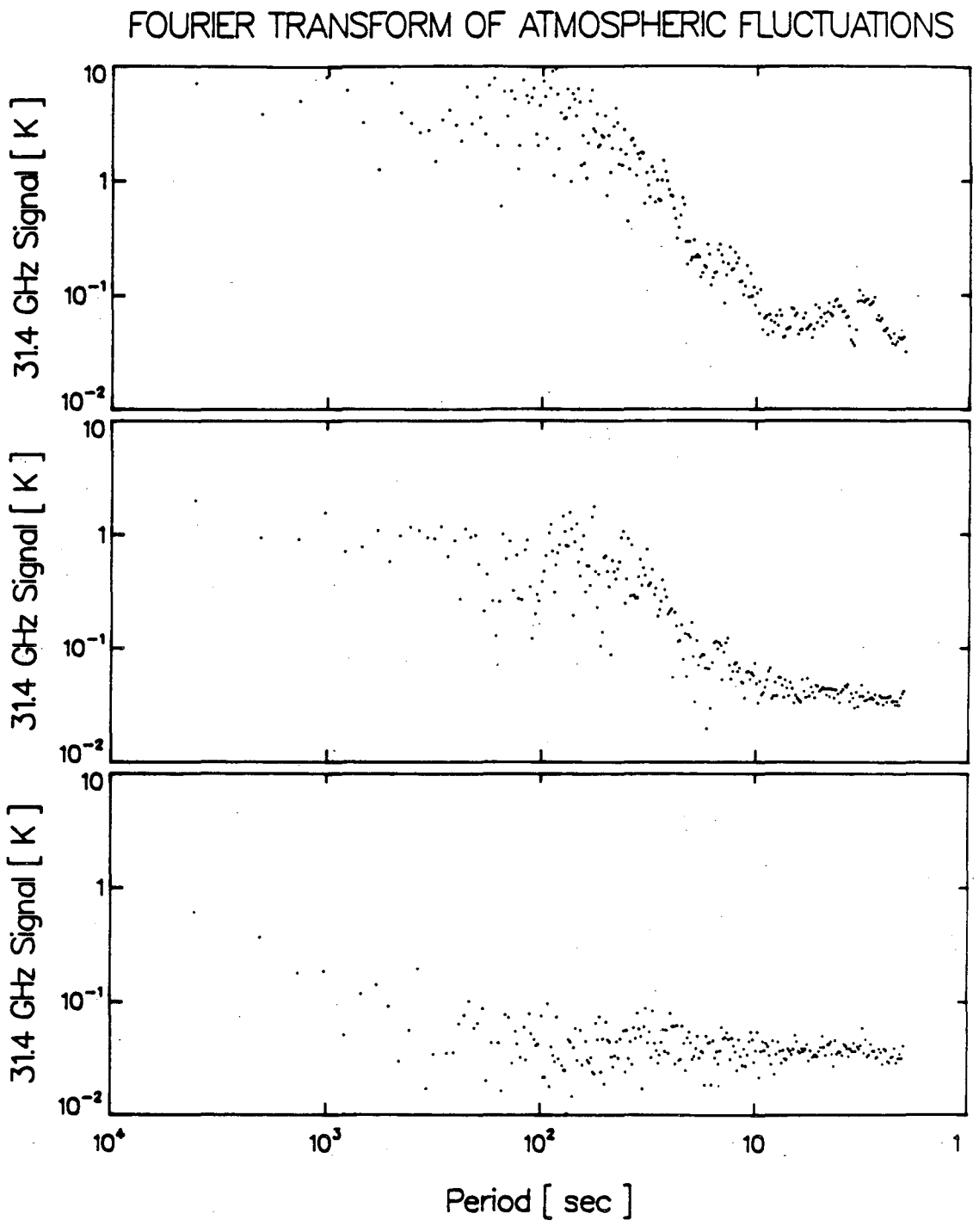

Figure 5. Sample Data from the 31.4 GHz Radiometer. Fourier Transform of data showing spectra of fluctuations. Data samples a, b, c, are the same as shown in figure 4.

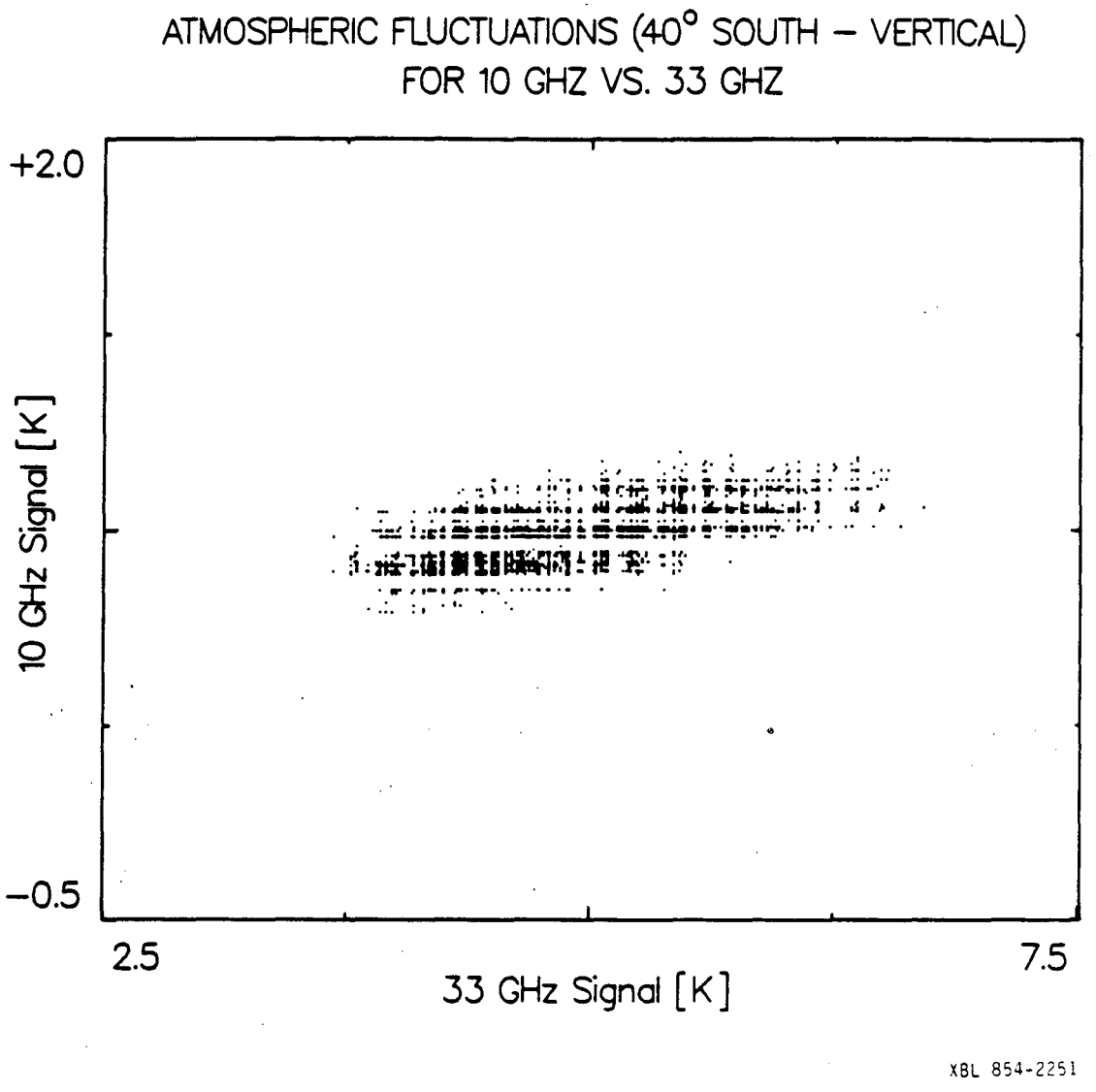

Figure 6. Correlation in Fluctuations of Atmospheric Signal From One Frequency to Another. a) 10 vs 33 GHz

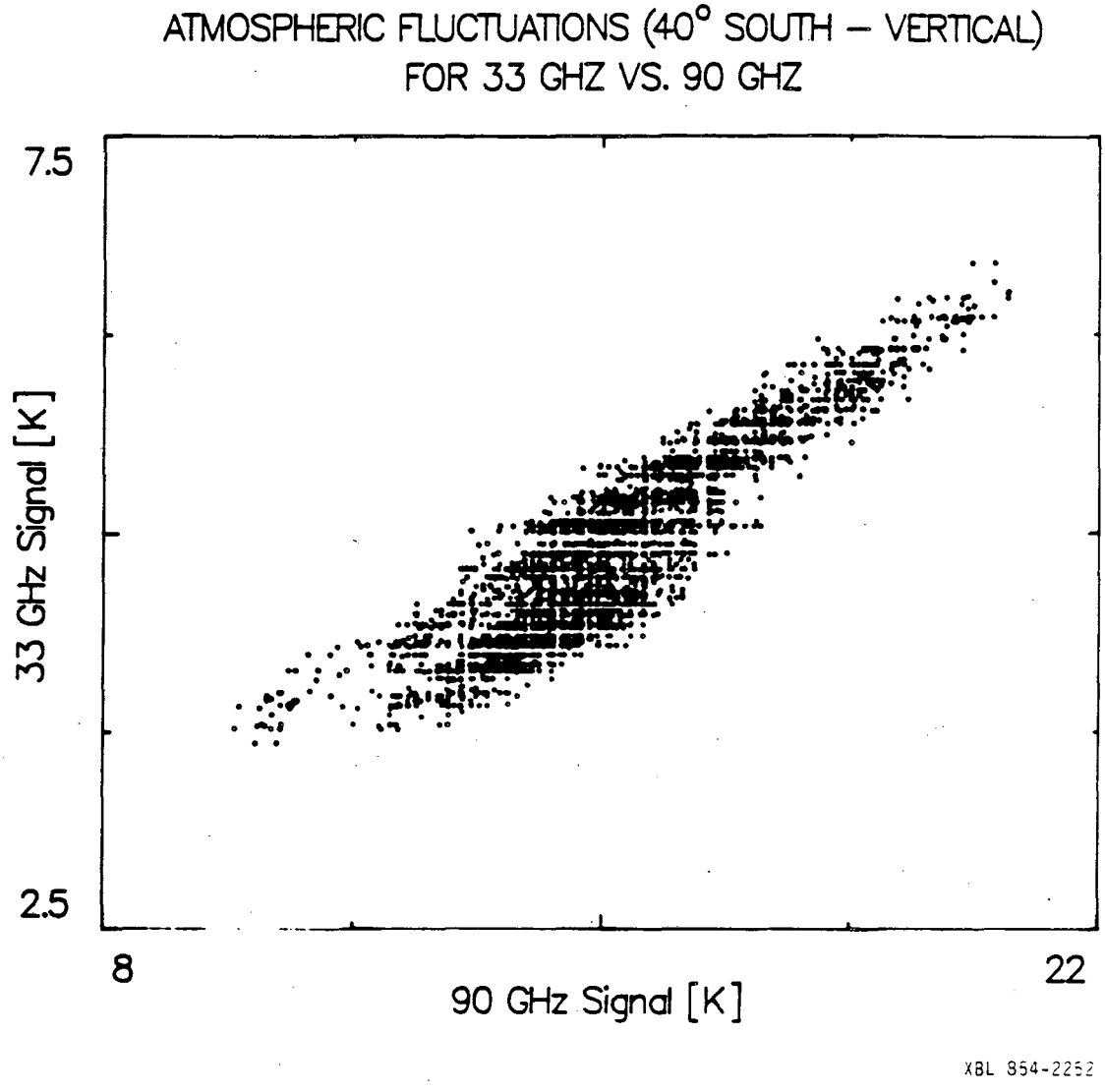

6 b) 33 vs 90 GHz

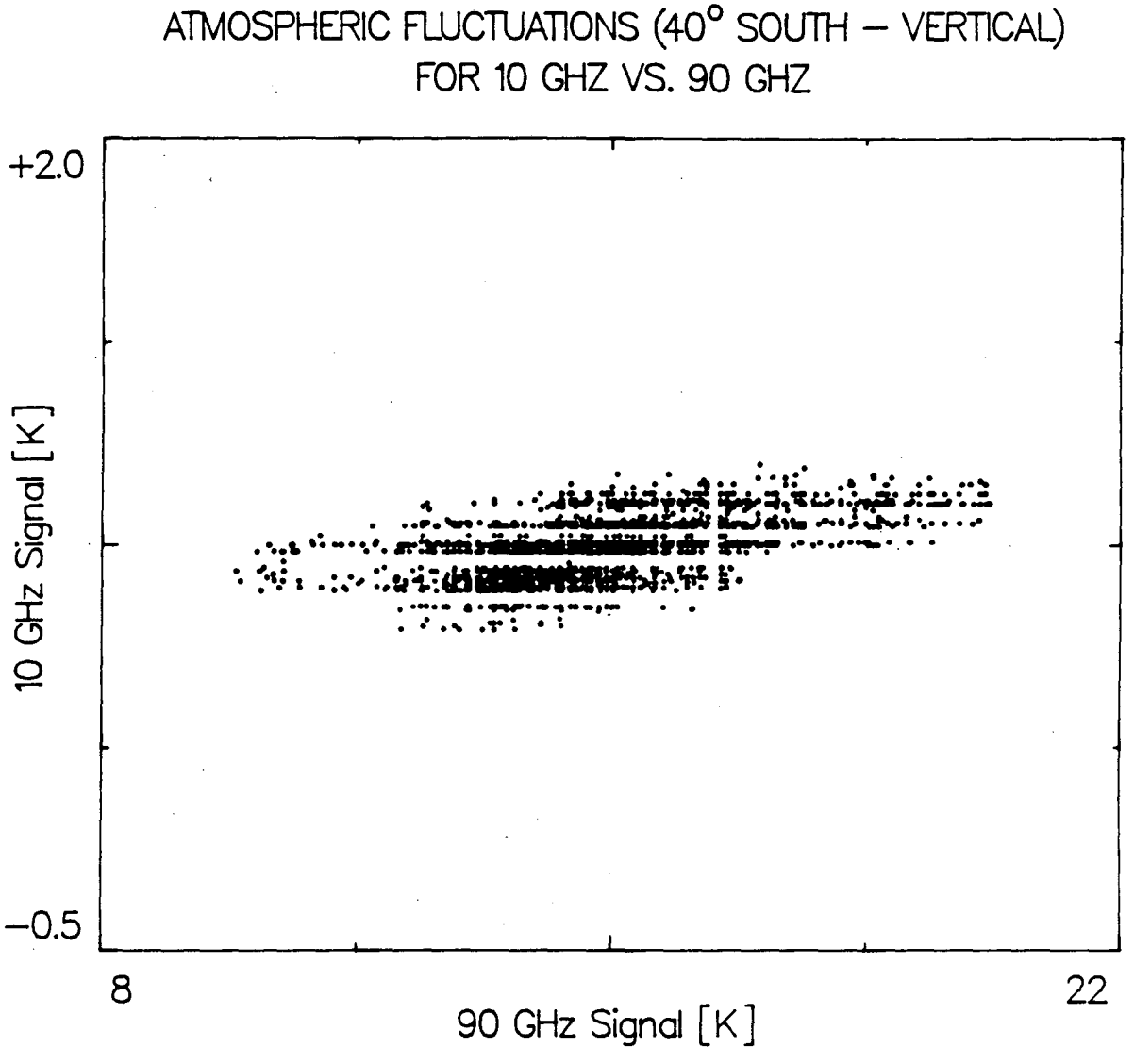

6 c) 10 vs 90 GHz

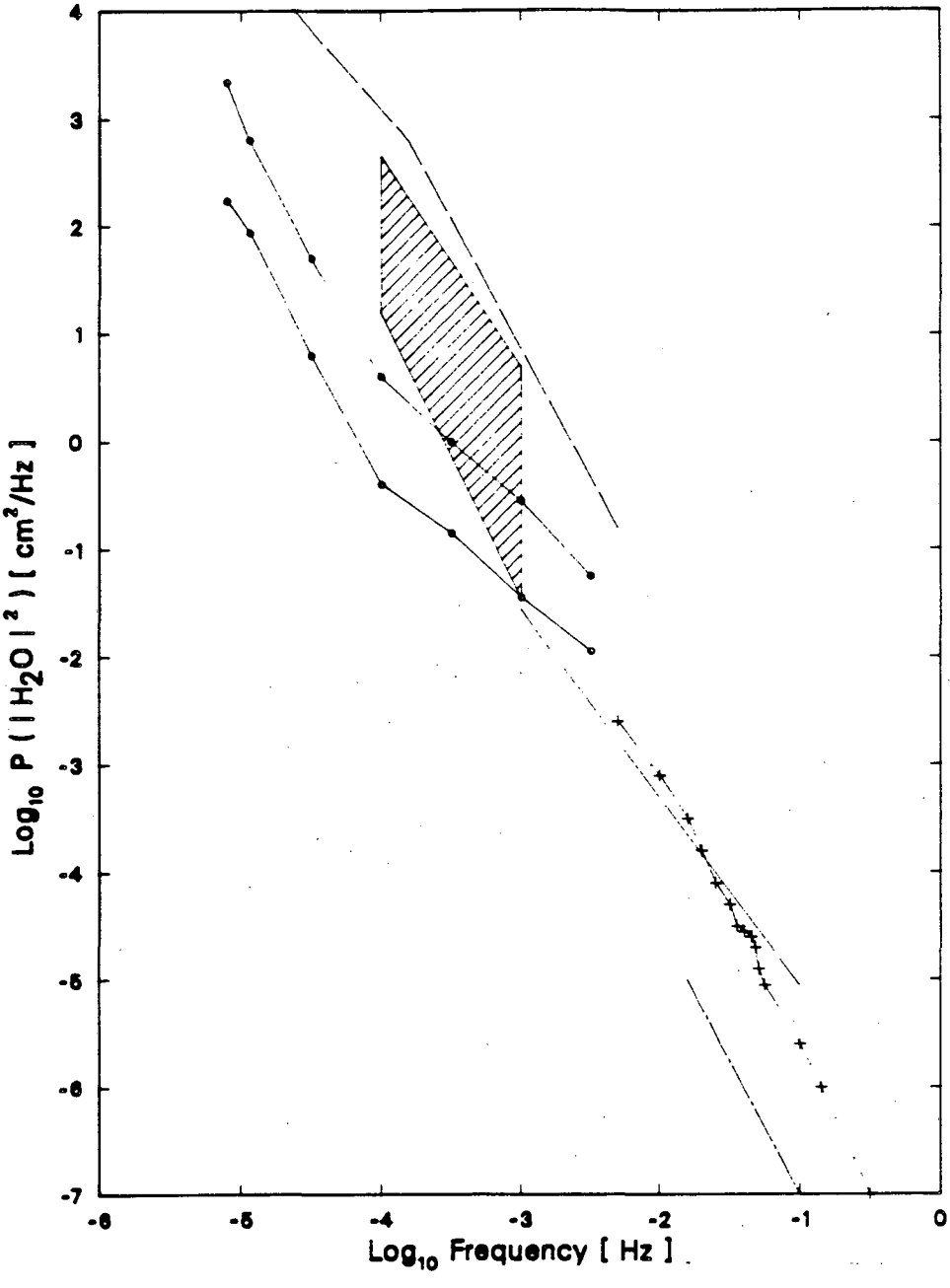

Figure 7. Power Spectra of Water Fluctuations. The dotted spectra are from *Hogg et al.*[1981]. The dashed line is the equivalent temporal spectrum inferred for the data of *Dravskikh and Finkelstein* [1979] according to the work of *Armstrong and Sramek* [1982] whose data are shown as the shaded box. The solid line is a sample of our data. Inclusion of all our data would produce a set of lines with slightly different slopes and relative heights of ± 50%. The +'s connected by the solid line are the converted phase (time delay) data of *Thompson et al.*[1975]. The dot-dash line indicates the optical data of *Shannon et al.*[1979].

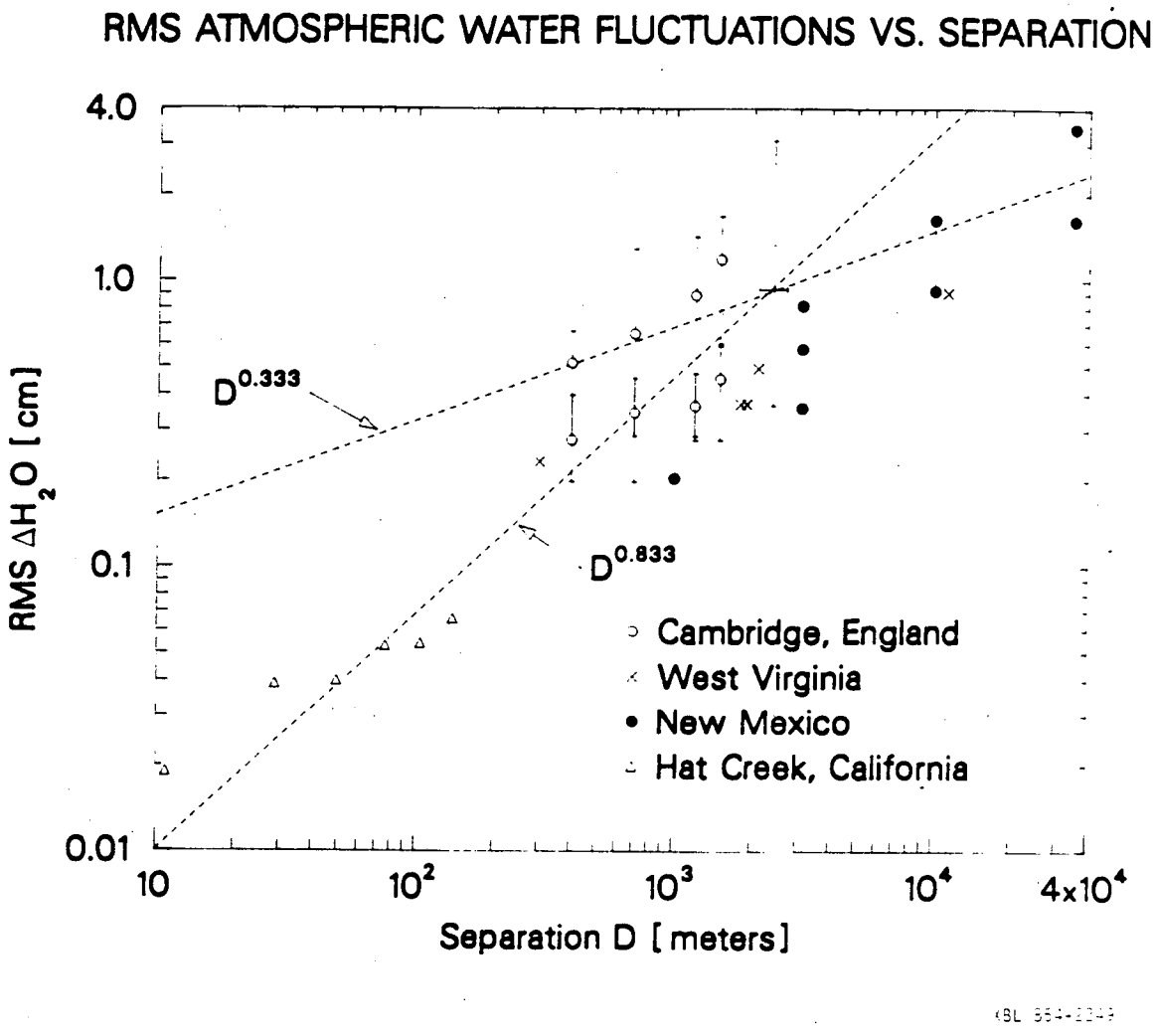

Figure 8. RMS Atmospheric Water Fluctuation versus Separation D. The dotted lines show the expected slopes for the two regimes. Unfortunately, the data come from different geographical locations and different seasons. The open circles show data from Cambridge, England; the higher values were obtained in the summer and the lower in winter. New Mexico is a drier site than England. Within their typical variation and accounting for geography the data are consistent with Kolmogorov turbulence theory.

This report was done with support from the Department of Energy. Any conclusions or opinions expressed in this report represent solely those of the author(s) and not necessarily those of The Regents of the University of California, the Lawrence Berkeley Laboratory or the Department of Energy.

Reference to a company or product name does not imply approval or recommendation of the product by the University of California or the U.S. Department of Energy to the exclusion of others that may be suitable.

LAWRENCE BERKELEY LABORATORY
TECHNICAL INFORMATION DEPARTMENT
UNIVERSITY OF CALIFORNIA
BERKELEY, CALIFORNIA 94720